Molecular Biology and Evolution, 2025, **42**, 1–16
https://doi.org/10.1093/molbev/msaf247
Advance access publication 26 September 2025
Discoveries

MBE OXFORD

Resolving the Stasis-Dynamism Paradox: Genome Evolution in Tree Ferns

Zuoying Wei [1,2,3,4,5], **Hengchi Chen** [4,5], **Chao Feng** [1,3,6], **Zengqiang Xia** [1,2,3], **Yves Van de Peer** [4,5,7,8,*], **Ming Kang** [1,3,6,*], **Jing Wang** [1,3,6,*]

[1]State Key Laboratory of Plant Diversity and Specialty Crops, South China Botanical Garden, Chinese Academy of Sciences, Guangzhou, China
[2]South China National Botanical Garden, Chinese Academy of Sciences, Guangzhou, China
[3]University of Chinese Academy of Sciences, Beijing, China
[4]Department of Plant Biotechnology and Bioinformatics, Ghent University, Ghent, Belgium
[5]VIB-UGent Center for Plant Systems Biology, Ghent, Belgium
[6]Key Laboratory of National Forestry and Grassland Administration on Plant Conservation and Utilization in Southern China, Guangzhou, China
[7]Department of Biochemistry, Genetics and Microbiology, University of Pretoria, Pretoria, South Africa
[8]College of Horticulture, Academy for Advanced Interdisciplinary Studies, Nanjing Agricultural University, Nanjing, China

***Corresponding authors**: **Emails:** yves.vandepeer@psb.vib-ugent.be; mingkang@scbg.ac.cn; wjing@scbg.ac.cn.
Associate editor: Kelley Harris

Abstract

The paradox of evolutionary stasis and dynamism—how morphologically static lineages persist through deep geological periods despite environmental fluctuations—remains unresolved in evolutionary biology. Here, we present chromosome-scale genomes for three ecologically divergent species (including both arborescent and nonarborescent growth forms) within Cyatheaceae, an ancient tree fern family characterized by morphological conservation dating back to the Jurassic era. Our results revealed substantial yet cryptically regulated genomic dynamism. A shared Jurassic whole-genome duplication (~154 Ma) conferred dual adaptive advantages: initially buffering tree ferns against Late Jurassic climatic extremes through retention of stress-response genes, and subsequently facilitating niche diversification and phenotypic innovation via lineage-specific repurposing of duplicate genes. Arborescent lineages preferentially retained duplicates involved in cell wall biogenesis, essential for structural reinforcement and lignification, while nonarborescent forms conserved paralogs linked to metabolic resilience and defense. Alongside slow substitution rates, we detected cryptic genome dynamism mediated primarily by bursts of transposable elements, leading to genome size variations, chromosomal rearrangements, and localized innovation hotspots with elevated evolutionary rates. The concerted expansion and expression of lignification-related genes, coordinated with light signaling components, suggest a potential evolutionary mechanism integrating light perception with shade adaptation and lignification, facilitating arborescent adaptation in angiosperm-dominated understories. Our findings redefine evolutionary stasis as a dynamic equilibrium, sustained by regulatory plasticity and localized genomic innovation within a conserved morphological framework. This study offers a novel genomic perspective on the long-term persistence and evolution of ancient plant lineages, demonstrating how regulated genomic dynamism enables adaptive diversification while sustaining morphological conservatism.

Keywords: evolutionary stasis, living fossil, tree fern, genome evolution, ancient polyploidy

Introduction

Ferns, one of the oldest extant lineages of vascular plants originating over 360 million years ago (Kenrick and Crane 1997; Schneider et al. 2004), have successfully colonized diverse biomes, thriving as both ecosystem engineers and shade-adapted specialists (Niklas et al. 1983; Testo et al. 2022; Wu et al. 2025). Their early innovations in lignin-based vasculature and secondary cell walls facilitated the colonization of terrestrial environments and the evolution of both arborescent (tree-like) and herbaceous growth forms, thereby underpinning subsequent plant diversification (Weng and Chapple 2010; Chomicki et al. 2017; Clark 2023; Ali et al. 2025). Despite their evolutionary success, the genomic mechanisms underlying the long-term persistence of ferns, particularly in morphologically static lineages termed as "living fossils," remain poorly understood.

A prevailing view attributes their persistence to genomic stasis, characterized by highly conserved karyotypes and exceptionally low nucleotide substitution rates (Soltis et al. 2002; Bomfleur et al. 2014; Schneider et al. 2015; Clark et al. 2016). This stasis paradigm stands in stark contrast to the pervasive genomic plasticity observed in seed plants (Wessler 2006; Chen et al. 2020; Tang et al. 2022; Long et al. 2024; Wang et al. 2025). However, emerging evidence from other fern clades reveals considerable karyotypic plasticity and dynamic genome evolution (Schneider et al. 2015; Wang et al. 2020; Marchant et al. 2022; Fernández et al. 2023; Fujiwara et al. 2023; Katayama et al. 2024), challenging the notion of genomic stasis and rekindling debate over whether fern evolution is fundamentally constrained by ancestral genomic architectures or instead driven by ongoing genomic innovation. Nevertheless, most existing evidence is derived from genomes of phylogenetically isolated taxa, highlighting a fundamental gap in our understanding of fern genome evolution across closely related species.

Received: May 29, 2025. **Revised:** September 9, 2025. **Accepted:** September 15, 2025

Resolving this stasis-dynamism paradox is particularly challenging due to the exceptionally large and complex nature of fern genomes. Ferns have notoriously colossal genome sizes (averaging 12.3 Gb and reaching up to 160 Gb in some species; Fernández et al. 2024) and unusually high chromosome numbers (mean = 40.5, maximum = 720; Khandelwal 1990). Such extraordinary genomic dimensions are largely the result of recurrent whole-genome duplications (WGDs) coupled with limited post-WGD genome downsizing (Haufler 2014; Clark et al. 2016; Marchant et al. 2022). These features have historically prevented the construction of high-quality fern genome assemblies, impeding our understanding of their evolutionary dynamics over deep time scales. To date, only a few chromosome-scale genomes have been published (Fang et al. 2022; Huang et al. 2022; Marchant et al. 2022; Rahmatpour et al. 2023; Qin et al. 2024; Shu et al. 2025). Most critically, the absence of comparative genomic frameworks among closely related fern lineages with ecological divergence has obscured our ability to determine whether long-term stasis is underpinned by genuine genomic stagnation or by covert genomic turnover.

Tree ferns in the order Cyatheales represent an ideal model system to interrogate the stasis-dynamism paradox in ferns. As the only extant ferns with arborescent growth, they are distinctive for iconic trunk-like stems crowned with expansive fronds (Fig. 1a) and exhibit remarkable morphological stasis dating back to the Jurassic era (Van Konijnenburg-Van Cittert 2002; Pryer et al. 2004). The family Cyatheaceae is the most species-rich clade within Cyatheales, accounting for over 90% of living tree fern species (PPG I 2016). Paradoxically, despite their ecological breadth and morphological variety, including both typical arborescent and derived nonarborescent forms lacking trunk-like stems (Wang et al. 2020), Cyatheaceae has experienced exceptionally low diversification rates over the past 145 million years (Korall et al. 2010; Loiseau et al. 2020). This unusual combination of pronounced morphological stasis, divergent growth forms, wide ecological distribution, and depressed diversification rates makes Cyatheaceae an excellent system to test whether long-term evolutionary persistence is driven by genomic stasis or by cryptic genomic dynamism.

Deciphering the evolutionary enigma of Cyatheaceae remains fundamentally constrained by the limitations of single-genome references. The recent assembly of *Alsophila spinulosa* provided initial insights into fern genome evolution (Huang et al. 2022); however, a single genome is insufficient to elucidate evolutionary dynamics across this ancient lineage. In the present study, we bridge this knowledge gap by assembling chromosome-level genomes for three ecologically divergent Cyatheaceae species: arborescent *Sphaeropteris brunoniana*, nonarborescent *Gymnosphaera denticulata*, and an improved assembly for the arborescent *Sphaeropteris lepifera*. By integrating comparative genomic and transcriptomic analyses, we uncovered an unprecedented degree of genomic dynamism in tree ferns despite their overall slow nucleotide substitution rates. Notably, we identified a Jurassic WGD event shared by all Cyathealean species that underpinned both their survival of Late Jurassic climatic extremes and subsequent Cenozoic adaptive diversification in tree ferns. Crucially, we found that arborescent versus nonarborescent lineages differentially retained ohnologs: arborescent species preferentially retained gene duplicates associated with cell wall biogenesis and lignification, whereas the nonarborescent lineage preserved more duplicates related to metabolism and defense. These contrasting retention patterns indicate an adaptive trade-off between structural reinforcement in arborescent lineages and metabolic resilience in nonarborescent lineages. We further observed substantial genome size variation and chromosomal rearrangements driven by lineage-specific bursts of transposable element (TE) proliferation, generating localized evolutionary hotspots with signs of positive selection. Finally, our results suggest a putative genomic framework linking light perception to shade adaptation and lignification pathways, a hallmark adaptation that enables tree ferns to thrive as understory plants beneath angiosperm-dominated canopies. Taken together, these findings resolve the stasis-dynamism paradox in tree ferns by demonstrating that it is the regulated genomic innovation—not static genome architecture—that underlies the long-term persistence and adaptive diversification of these ancient lineages in the face of geological and environmental upheavals.

Results

Genome Assemblies and Annotations

We assembled high-quality, chromosome-scale genomes for three ecologically divergent species: *S. brunoniana*, *G. denticulata*, and *S. lepifera*. These assemblies were generated by combining PacBio HiFi long reads, Illumina short reads, and high-throughput chromosome conformation capture (Hi-C) data. The final genome assemblies ranged from 2.54 Gb in *S. brunoniana* (contig N50 = 6.09 Mb) to 6.25 Gb in *G. denticulata* (contig N50 = 7.57 Mb; Table S1). Hi-C scaffolding anchored ~98% of each assembled genome to chromosomes, revealing lineage-specific karyotypic differences in haploid chromosome number ($n = 68$ to 69) (Figs. S1 and S2). Specifically, both *S. brunoniana* and *S. lepifera* retain the typical 69 chromosomes (Rice et al. 2015), whereas *G. denticulata* carries a reduced complement of $n = 68$ (Figs. 1b and S2c). This chromosome reduction in *G. denticulata* is consistent with its proposed role as one progenitor of the allotetraploid *G. metteniana* ($n = 137$; Nakato 1989), as the other progenitor likely retained the ancestral chromosome number of $n = 69$ (Wang et al. 2020). BUSCO (Benchmarking Universal Single-Copy Orthologs) assessment with the Eukaryota_odb10 database recovered 87.5%, 97.2%, and 98.0% of core eukaryotic genes in *S. lepifera*, *S. brunoniana*, and *G. denticulata* assemblies, respectively (Table S1). Using a combination of ab initio prediction, homology searches, and RNA-seq data, we annotated 33,993, 39,097, and 40,140 high-confidence protein-coding genes in *S. lepifera*, *S. brunoniana*, and *G. denticulata*, respectively (Table S1). Repetitive sequences (largely TEs) accounted for ~81.82%, 81.89%, and 87.08% of each genome, respectively (Table S2), indicating that repeats are the major contributors to their large genome sizes.

A Jurassic WGD as an Adaptive Substrate

Through integrated comparative genomic analyses, including synteny mapping, K_S age distribution, and phylogenomic reconciliation, we identified a single ancient WGD event (~154 Ma) shared by all studied Cyatheaceae species. Analysis of K_S distributions for both the whole paranome (the complete set of duplicated genes within each genome) and syntenic anchor pairs (duplicated genes resulting from large-scale duplication events and still residing in recognizable duplicated genomic regions) revealed a consistent peak at $K_S \approx 0.3$ (Fig. 2a). Exponential-lognormal mixture modeling

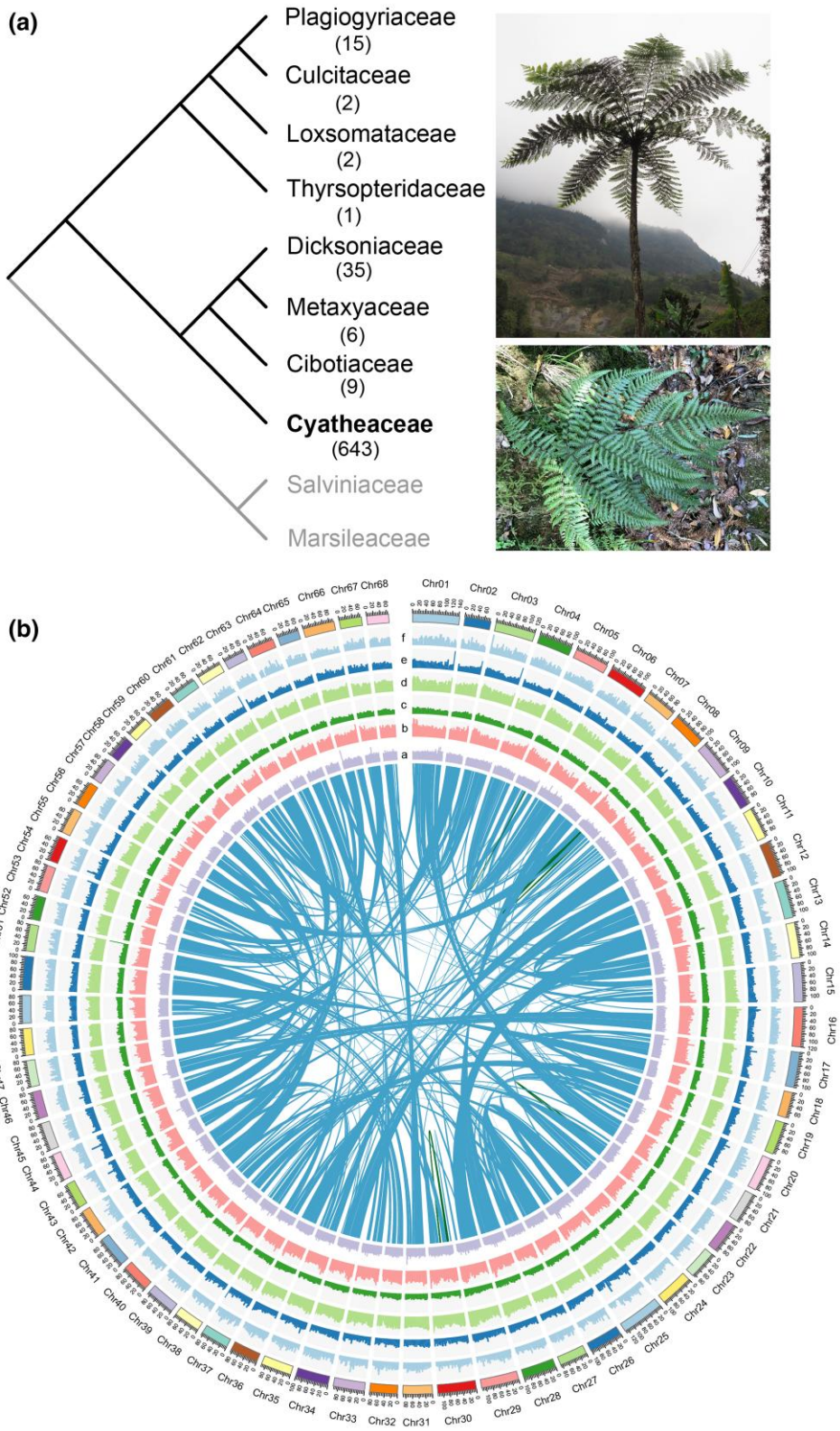

Fig. 1. Phylogenetic relationship and genome features. a) Phylogenetic relationship within the order Cyatheales (clade denoted with black lines), with species numbers of each family indicated in parentheses. The right panel displays two representative growth morphologies: the upper image shows the arborescent morphology of *S. brunoniana*, while the lower image depicts the nonarborescent morphology of *G. denticulata*. b) The genomic landscape for *G. denticulata*. Tracks "a to f" represent tandem repeat density, LTR/*Gypsy* density, LTR/*Copia* density, TE density, GC content, and gene density, respectively. The inner lines represent both interchromosomal (blue) and intrachromosomal (green) synteny. The genomic landscapes of *S. brunoniana* and *S. lepifera* can be found in Figure S1.

(ELMM) and Gaussian mixture modeling (GMM) analyses corroborated the presence of only one recent peak (Fig. S3). These consistent K_S peaks strongly suggest an ancient polyploidy event among the tree fern genomes, likely with similar age. We further found that numerous large intragenomic syntenic blocks are preserved for each Cyatheaceae

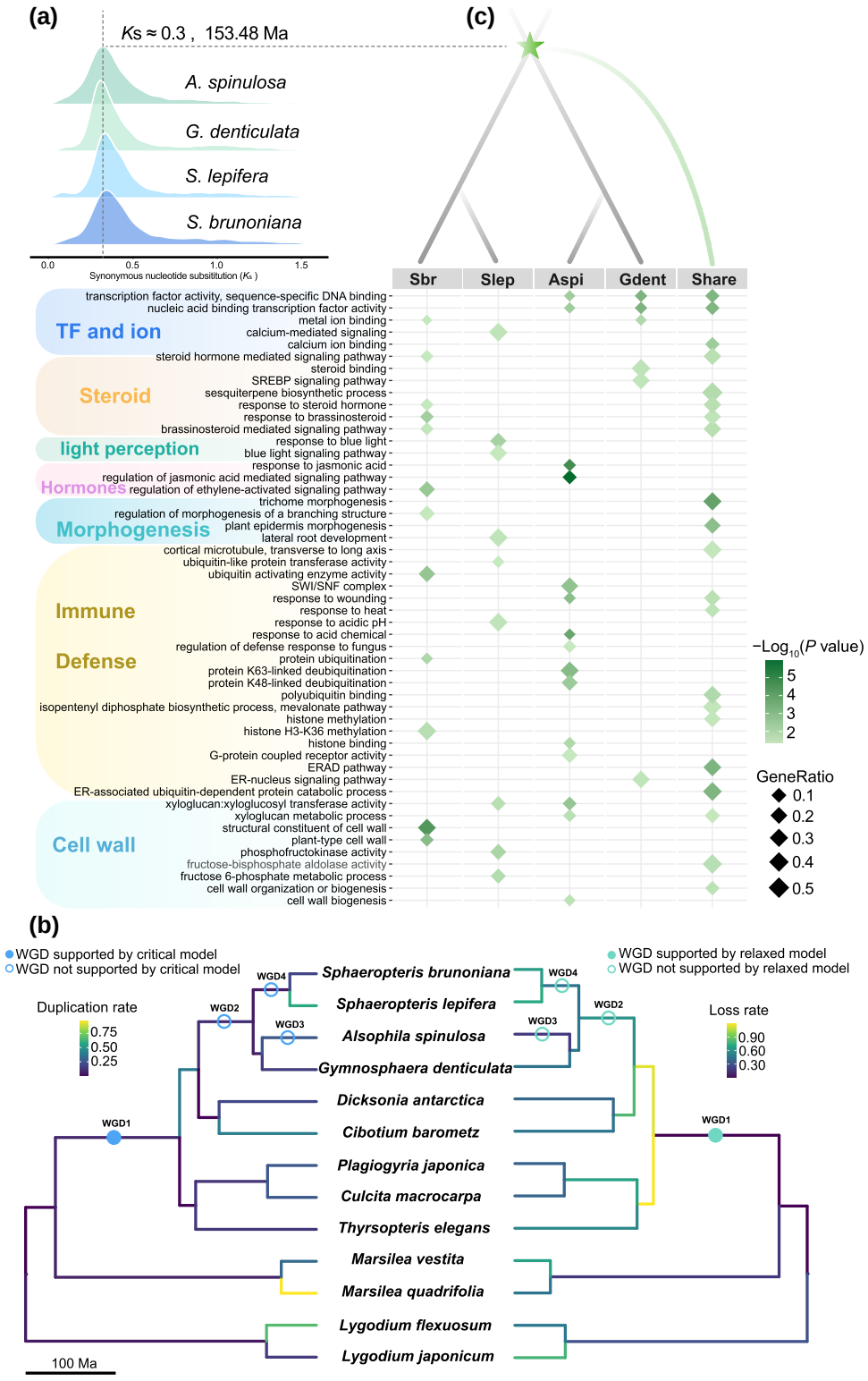

Fig. 2. WGD events and subsequent gene retention across the four Cyatheaceae species. a) Ridgeline plot showing the K_S distribution for paralogous gene pairs of the four Cyatheaceae species. b) The four putative WGD events tested in the "relaxed" and "critical" models on a species chronogram, in which the solid circle in blue on the left cladogram (for the critical branch-specific model) and in light blue on the right cladogram (for the relaxed branch-specific model) indicate support in terms of Bayes Factor, while the hollow circles denote lack of support. See text for details. c) Different patterns of GO enrichment for genes commonly retained by the four species (share) and genes preferentially retained by each species (Sbr, *S. brunoniana*; Slep, *S. lepifera*; Aspi, *A. spinulosa*; Gdent, *G. denticulata*) following WGD. The green star indicates an ancient Cyathealean WGD event.

species and pairwise intergenomic syntenic ratios are consistently delineated as 2:2 (Figs. S4–S7), substantiating the occurrence of an ancient polyploidy event in the genome of each Cyatheaceae species.

To clarify whether the inferred WGD was lineage-specific or shared across Cyathealean species, we further employed two complementary methods: the substitution rate-corrected K_S implemented in wgd v2 (Chen et al. 2024), and the gene

tree-species tree reconciliation-based phylogenomic method in WHALE (Zwaenepoel and Van de Peer 2019). Both approaches consistently supported a single ancient WGD event shared across Cyatheales species (Figs. 2b and S8 and Table S3), with no indication of additional lineage-specific or nested ancient polyploidy events. Fossil-calibrated molecular dating placed this WGD event in the Late Jurassic (~154.49 Ma; Fig. S9a), a period characterized by pronounced climatic fluctuations, including rising global temperatures and severe regional aridification (Yi et al. 2019; Judd et al. 2024; Fig. S9b).

Consistent with these environmental stresses, genes retained from this WGD showed significant enrichment in pathways associated with abiotic stress resilience, notably heat and drought stress responses (Fig. 2c and Table S4). Analysis of ohnolog retention revealed divergent patterns between growth forms: arborescent lineages preferentially preserved gene duplicates in cell wall biogenesis pathways (Fig. 2c and Tables S5–S7), while the nonarborescent *G. denticulata* selectively retained more duplicates associated with sterol metabolism (Fig. 2c and Table S8).

Genomic Plasticity Despite Syntenic Conservation

Despite originating over 218 Ma (95% HPD: 149 to 297 Ma; Fig. S10), Cyatheaceae genomes display strikingly conserved macrosynteny, maintaining over 90% collinearity among the studied species (Fig. S7 and Table S9). Comparative analysis showed that synteny decay rates in Cyatheaceae are markedly lower compared with other fern orders such as Polypodiales and Salviniales (Fig. 3a and b). Analysis of absolute substitution rates of 583 low-copy nuclear orthologues revealed that Cyatheaceae genomes evolve exceptionally slowly (0.42 to 1.08×10^{-9} substitutions per site per year), ~3-fold slower compared with other ferns (Fig. 3c and Table S10). Both synonymous (d_S) and nonsynonymous (d_N) substitution rates in Cyatheaceae are significantly reduced, as shown by a least significant difference test ($P < 0.05$; Figs. 3d and S11 and Table S11).

The activity of TEs emerges as the primary force reshaping Cyatheaceae genomes despite their slow sequence evolution and conserved synteny. This is substantiated by a 2.5-fold variation in genome size (Table S1) among the three newly assembled species. Long-terminal repeat retrotransposons (LTR-RTs), particularly Ty3/*Gypsy* and Ty1/*Copia* elements, represent the most prevalent class and serve as the main contributors to interspecific genome size disparity (Fig. 4a and Table S12). The cumulative lengths of Ty3/*Gypsy* and Ty1/*Copia* were considerably shorter in *S. brunoniana* (0.82 and 0.77 Gb, respectively) than in *S. lepifera* (1.51 and 1.72 Gb) and *G. denticulata* (1.59 and 1.00 Gb; Table S12). Although intact Ty3/*Gypsy* and Ty1/*Copia* elements accumulated steadily over the last ~20 Ma, their insertion numbers are markedly reduced in *S. brunoniana* relative to other Cyatheaceae species with larger genomes (Fig. 4b). We detected a higher solo-LTR to intact-LTR ratio in *S. brunoniana* (6.07), compared with *S. lepifera* (1.74), *G. denticulata* (3.96) and *A. spinulosa* (5.88) (Table S13). Notably, genome reduction in *S. brunoniana* is also reflected in significantly shorter intergenic regions relative to closely related species (Wilcoxon test, $P < 0.05$) (Fig. 4c).

We identified lineage-specific chromosomal rearrangements. Arborescent species (*S. brunoniana* and *S. lepifera*) display reciprocal translocations involving chromosomes Chr01, Chr03, Chr62, Chr67, and Chr69 (Fig. 4d). In contrast, the nonarborescent *G. denticulata* underwent independent large-scale chromosome fusions involving Chr41, Chr50, and Chr66 (Figs. 4d and S12), driving substantial karyotypic diversification. This resulted in the retention of 1,094 post-fusion genes, compared with 9,690 homologs (HGs) located on nonrearranged chromosomes. Notably, the breakpoints of these *G. denticulata* fusions were significantly enriched for TEs relative to the genomic background (Wilcoxon test, $P < 0.0001$; Fig. S13).

Genome Dynamism Facilitating Stress and Defense Resilience

To evaluate the evolutionary consequences of the independent chromosome fusion events observed in *G. denticulata*, we compared evolutionary rates and expression profiles of genes located on the fused chromosomes versus nonrearranged chromosomes. Postfusion genes located on chromosomes Chr41 and Chr66 in *G. denticulata* showed significantly elevated synonymous substitution rates (d_S; Wilcoxon test, $P < 0.0001$; Fig. 5a), whereas genes on Chr50 exhibited increased nonsynonymous-to-synonymous substitution ratios (ω; Fig. 5a). Additionally, post-fusion genes displayed significantly higher expression levels across various tissues (roots, stems, and fronds; Fig. 5b and c), and were particularly enriched in metabolic pathways involved in defense compound synthesis and plant–pathogen interaction (Fig. 5d).

Gene family analyses revealed 1,777 expanded versus 159 contracted families in Cyatheaceae (Fig. 3c). Expanded gene families showed significant functional enrichments in categories critical for environmental adaptation, notably jasmonic acid signaling, sterol biosynthesis, and cell wall organization (Figs. 5e and S14, and Tables S14 and S15). Notably, many stress-responsive genes tend to be arranged in tandem arrays along chromosomes (Fig. S15). One representative example is a cluster of 2,3-oxidosqualene cyclase (OSC) genes located on chromosome 58 of *S. lepifera* (Fig. 5f). This cluster forms a putative terpenoid biosynthetic gene cluster and exhibits signatures of positive selection (Figs. S16 and S17).

Coordinated Genomic Regulation of Arborescence

To further explore the genomic basis of arborescence, we performed detailed comparative genomic and transcriptomic analyses. Arborescent Cyatheaceae species exhibit substantial expansions of NAC transcription factors—key regulators of secondary cell wall formation and vascular tissue biosynthesis, which are markedly reduced in the nonarborescent *G. denticulata* (Fig. S18). Crucially, NAC-mediated secondary wall thickening is likely regulated by blue light signaling, which also modulates shade tolerance (Gommers et al. 2013; McCahill and Hazen 2019; Fig. 6a). In agreement with this proposed light-dependent mechanism, comparative genomic analyses revealed a coordinated expansion of genes related to shade response and secondary cell wall formation in tree ferns. Specifically, we observed significant expansion and retention of both cryptochrome (*CRY*) and ethylene-responsive *EIN3/EIL1* transcription factor gene families (Fig. 6b and Table S16). While nonarborescent *G. denticulata* retains more copies of some upstream lignin biosynthesis genes (e.g. *C4H* and *F5H*), it paradoxically possesses fewer copies of most key lignin polymerization enzymes compared with arborescent lineages (Fig. 6c). Strikingly, arborescent lineages possess roughly twice the copy number of the critical polymerization enzymes—peroxidase (*POX*) and laccase (*LAC*)—

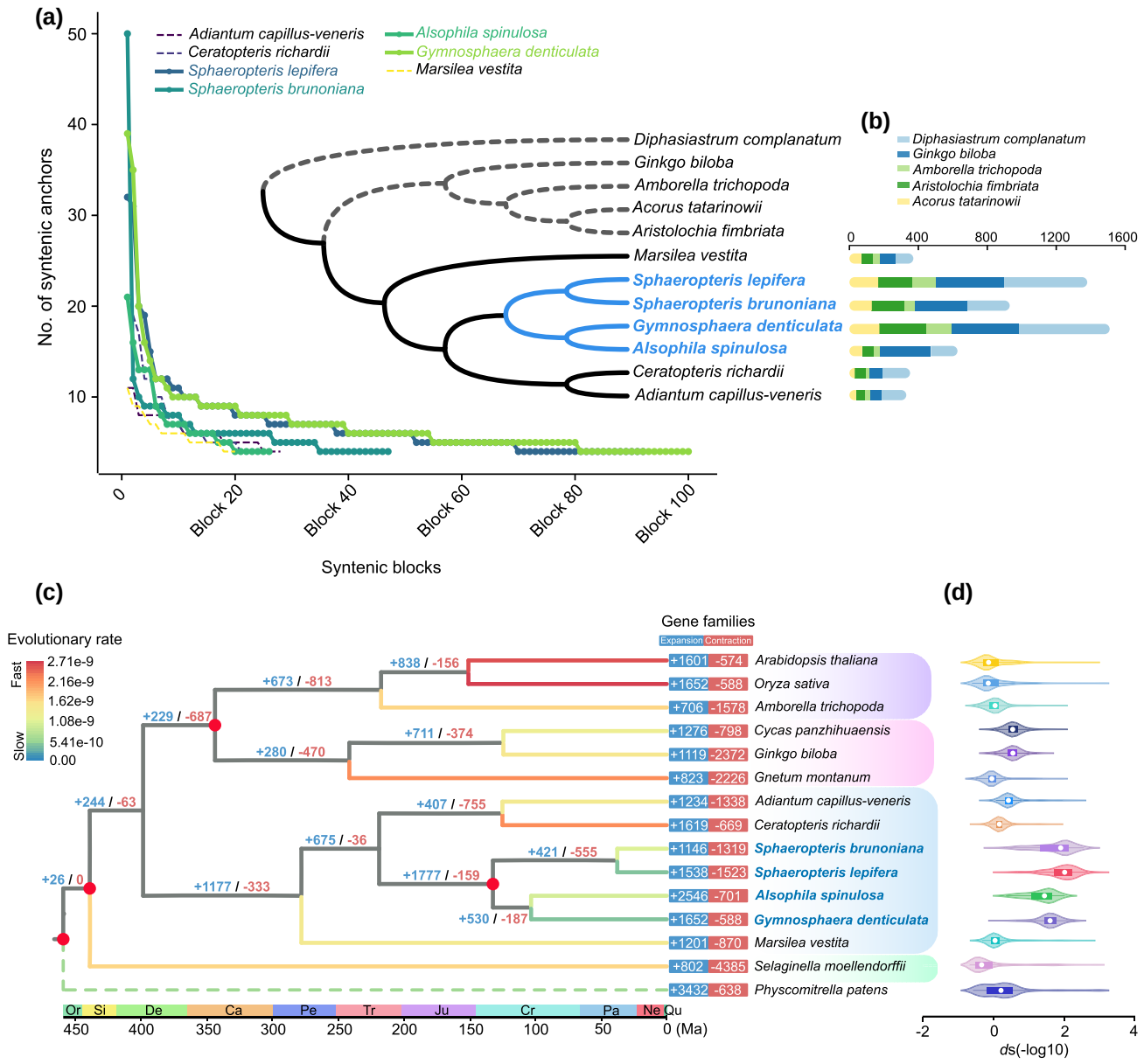

Fig. 3. Genomic conservation and decelerated molecular evolution. a) Comparison of "syntenic block size" decay among different fern species. b) Distributions of syntenic gene retention from the five outgroup species in seven ferns with chromosome-level assembly shown as colored bars. c) Phylogenetic tree of 15 species showing divergence times and the evolution of gene family sizes. All the species sequenced in the present study are highlighted in blue color. The solid circles in red represent the fossil and secondary calibration nodes. The numbers labeled on the branch and in the bar on the right panel correspond to the amount of expanded (blue) and contracted (red) gene families. Branches are colored according to the absolute substitution rate (the number of substitutions per site per year). In general, red shifts indicate an increased substitution rate; the opposite is true for blue shifts. d) Violin plots with box plots show the d_S values (–log10 scale) for each species. The box-plot elements are defined as: white dots, median; box limits, first and third quartiles; whiskers, 1.5× interquartile range.

compared with *G. denticulata* (Fig. 6c). Critically, arborescent lineages exhibit robust expression of *POX/LAC* genes in stems, stipes, and fronds, contrasting sharply with only weak expression in roots of *G. denticulata* (Fig. S19). Similar contrasting expression patterns were observed for the cellulose synthase/cellulose synthase-like (*CesA/Csl*) genes (Fig. S20).

Discussion

The evolutionary stasis-dynamism paradox—how morphologically static lineages like tree ferns persist through deep time despite minimal apparent change—has remained unresolved. Integrating chromosome-level comparative genomics and transcriptomic analyses of ecologically divergent tree ferns, we find that ultralow nucleotide substitution rates coexist with cryptic genomic dynamism driven by a sophisticated interplay of ancient polyploidy, TE activity, and regulatory innovation. These findings redefine fern "stasis" not as genomic stagnation but as a dynamic equilibrium between internal genomic plasticity and external morphological constraint—a balance that has sustained Cyatheaceae persistence across geological epochs.

Jurassic Whole-Genome Duplication as a Phased Genomic Reservoir

The evolutionary significance of polyploidy in ferns has been debated for decades (Klekowski and Baker 1966; Soltis et al.

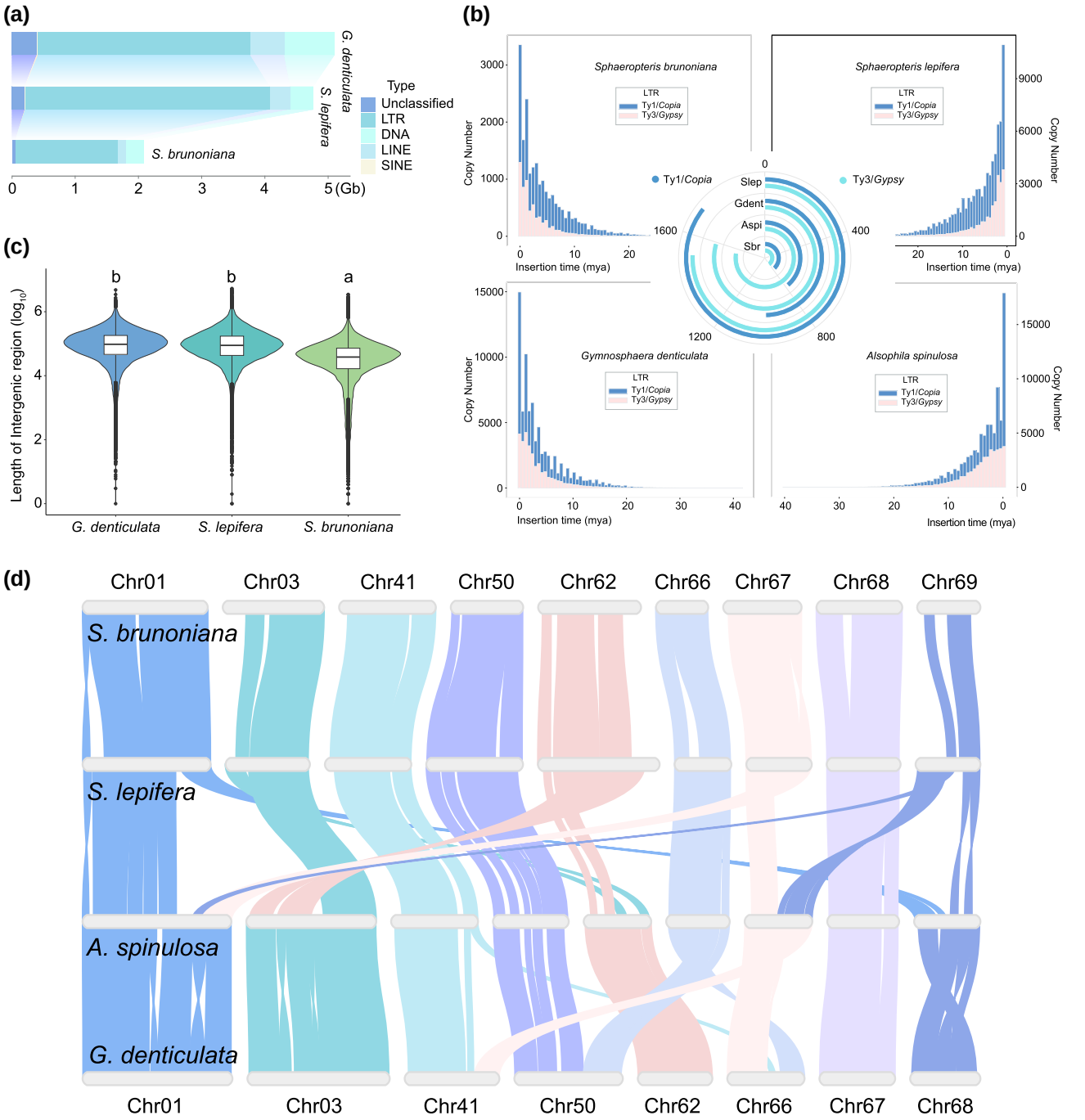

Fig. 4. Genomic dynamism within Cyatheaceae. a) Total length of each type of TE in each species. b) Distribution of insertion times for Ty3/*Gypsy* and Ty1/*Copia* elements in the four Cyatheaceae species. The circular barplot shows the total length of Ty3/*Gypsy* (cyan) and Ty1/*Copia* (blue) elements in *S. lepifera* (Slep), *G. denticulata* (Gdent), *A. spinulosa* (Aspi), and *S. brunoniana* (Sbr). c) Violin plots with overlaid box plots illustrating the distributions of intergenic region lengths for each species. Box-plot elements are defined as follows: center line, median; box limits, first and third quartiles; points, outliers; whiskers, 1.5 × interquartile range. Significance levels were determined using Wilcoxon tests. Shared letters above violins indicate no significant difference in intergenic region length between species, while different letters denote significant differences. d) Synteny of chromosomes with macrorearrangements across the four Cyatheaceae species. Each horizontal bar represents a chromosome, with chromosome IDs of *S. brunoniana*, *S. lepifera*, and *A. spinulosa* labeled at the top and those of *G. denticulata* labeled at the bottom. Syntenic blocks are colored based on their correspondence to *S. brunoniana* chromosomes.

2015; Huang et al. 2020; Van de Peer et al. 2021). Previous studies relying on transcriptomes or partial genome assemblies yielded conflicting hypotheses regarding WGD in tree ferns, with proposed scenarios ranging from a single shared polyploidy to multiple independent WGD events occurring at different times (Huang et al. 2020, 2022; Chen et al. 2022; Pelosi et al. 2022). By leveraging multiple chromosome-level genome assemblies and an integrated phylogenomic framework, our analyses resolved these discrepancies. We uncovered evidence for a single Jurassic WGD event (~154 Ma) shared across the Cyathealean lineages and further elucidated its adaptive significance in tree fern evolution.

Our findings demonstrate that the Jurassic WGD event acted initially as a buffer against Late Jurassic environmental stresses and later as a source of phenotypic innovation and ecological diversification. During the Upper Jurassic, when

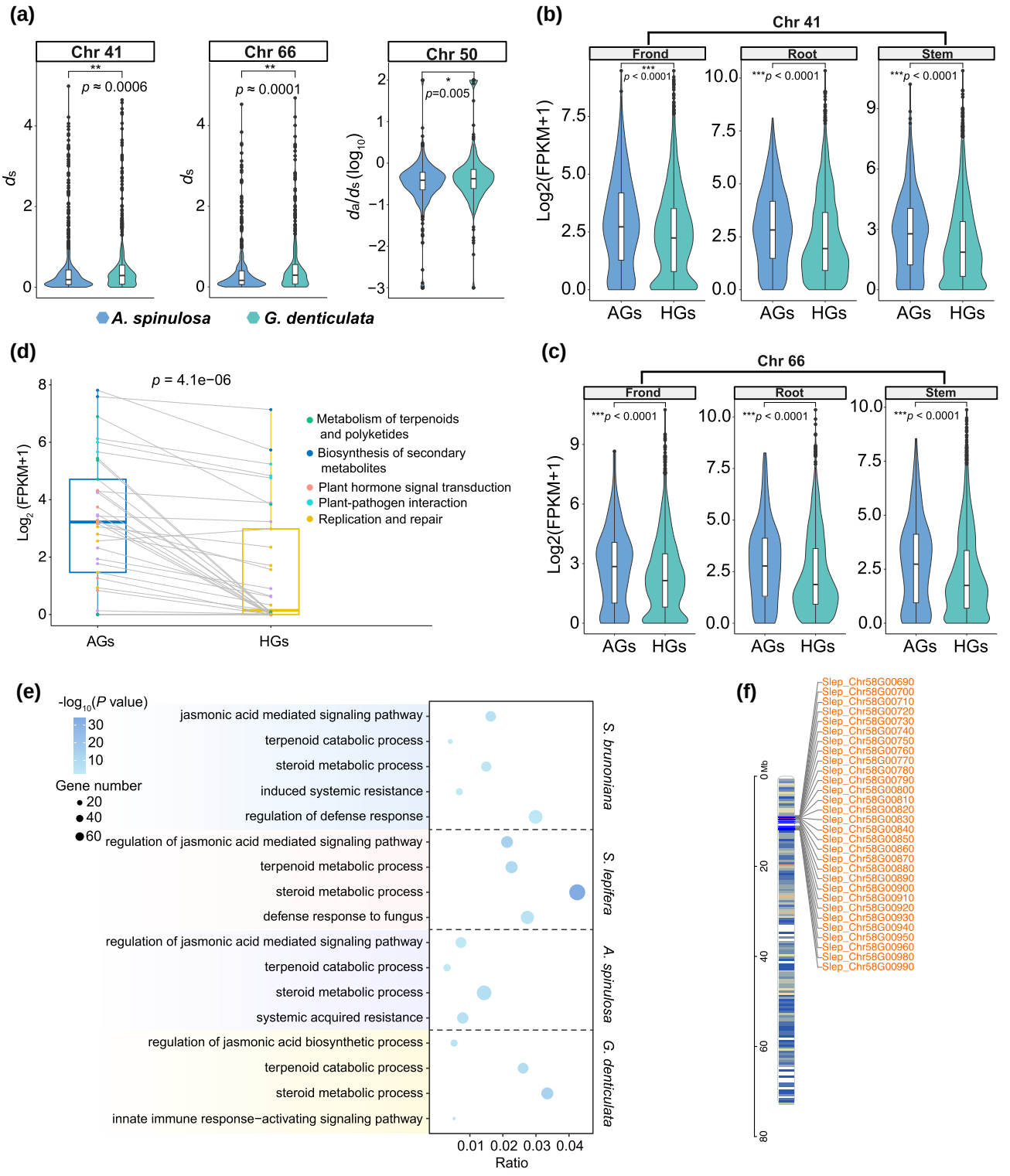

Fig. 5. Genomic consequences of lineage-specific fusion events and expanded gene families in Cyatheaceae. a) Comparison of nucleotide substitution rates and selection pressure between genes located on the three fused chromosomes (i.e. Chr41, Chr50, and Chr66) in *G. denticulata* and their orthologs located on the pre-fusion chromosomes of *A. spinulosa*. b, c) Gene expression comparison across frond, root, and stem tissues between genes from the fused chromosomal regions (AGs) of Chr41 and Chr66 and their homologs (HGs) on nonrearranged chromosomes in *G. denticulata*. Expression values are scaled by $\log_2$ (FPKM + 1). d) KEGG annotation of genes distributed in the fusion fragments and comparison of their expression levels with homologous genes in the nonrearranged region in *G. denticulata*. Dots with different colors represent genes involved in different biological processes. e) GO enrichment of significantly expanded gene families ($P < 0.05$) in each species. f) The OSCs gene cluster on chromosome 58 of *S. lepifera*. In a–c, box-plot elements are defined as follows: center line, median; box limits, first and third quartiles; points, outliers; whiskers, 1.5x interquartile range. Wilcoxon tests were conducted for significance evaluation. Asterisks represent significant differences (***$P < 0.0001$; **$P < 0.001$; *$P < 0.01$).

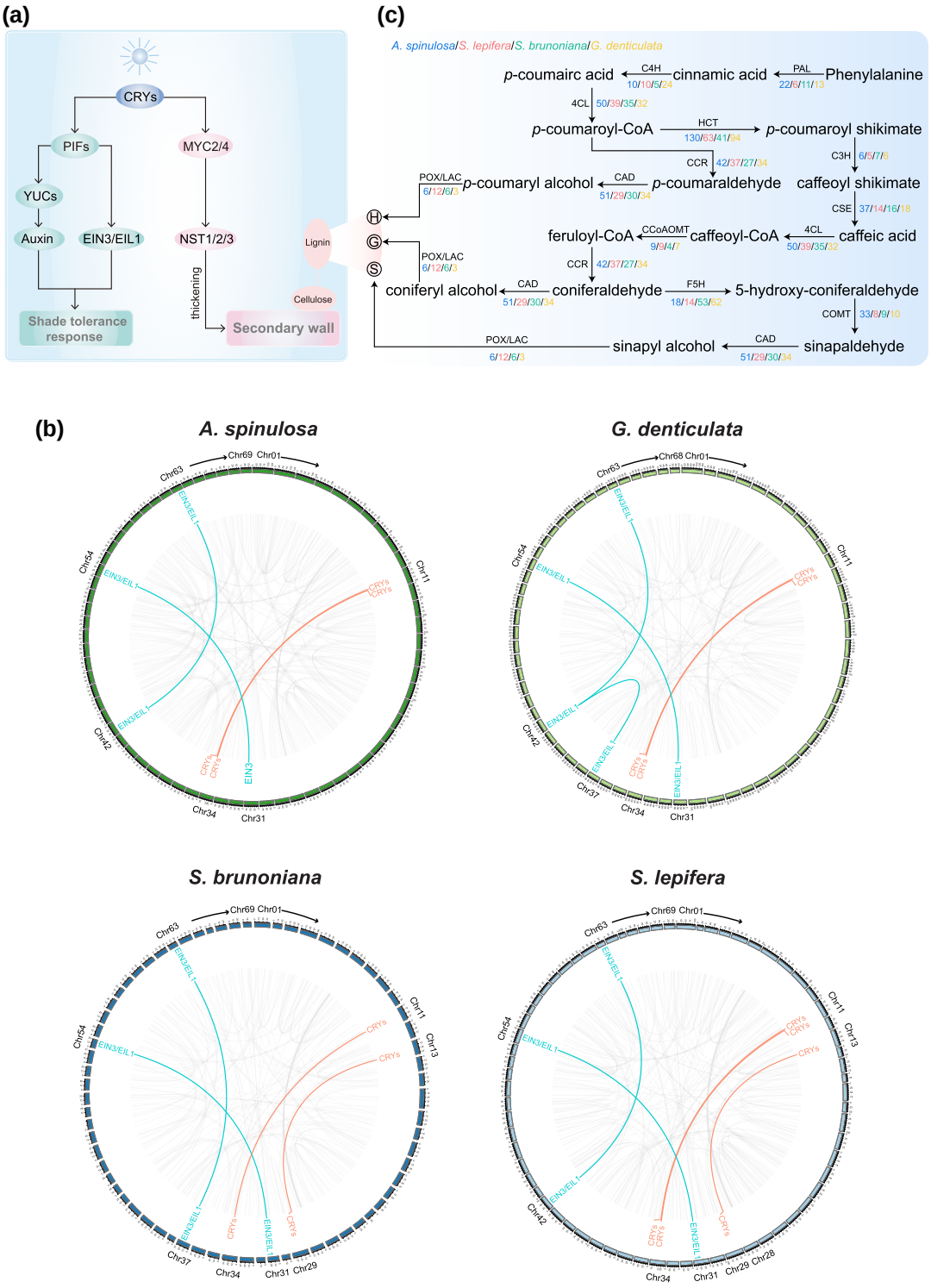

Fig. 6. Shade response and secondary cell wall formation in tree ferns are mediated by distinct regulatory modules and gene retention patterns. a) A simplified gene regulatory network mediating shade-adaptation response and secondary wall thickening, modified from Gommers et al. (2013) and McCahill and Hazen (2019). b) Syntenic relationships of genes involved in light perception and signaling across the four Cyatheaceae species. Different colors represent different genes derived from the Cyathealean WGD event. c) The number of genes involved in the lignin biosynthetic pathway across the four Cyatheaceae genomes. Numbers are colored according to the species color scheme shown on the top.

global temperatures rose and aridity became widespread (Yi et al. 2019; Judd et al. 2024), the retained gene duplicates from this ancient polyploidy event show significant enrichment in heat- and drought-response functions. This pattern suggests that WGD-derived genetic redundancy contributed to physiological robustness, allowing tree ferns to endure extreme environmental conditions while maintaining morphological stasis over geological timescales. The lineage-specific divergence in the retention of WGD-derived genes further underscores how this single polyploidy event facilitated ecological diversification: arborescent tree ferns have preferentially retained ohnologs involved in secondary cell wall biosynthesis and lignification, whereas nonarborescent species have instead preserved ohnologs related to sterol metabolism and chemical defense—traits critical for water conservation

and biotic resistance (Tong et al. 2022). These contrasting retention profiles indicate that the Jurassic WGD served as a versatile genetic toolkit that was selectively deployed by different tree fern lineages based on their ecological niches.

In seed plants, the development of woody trunks depends on robust secondary cell walls composed of lignin, cellulose, and hemicellulose (Wolter 1973). For instance, woody bamboos exhibit elevated copy numbers of cellulose- and lignin-synthesis genes compared with herbaceous relatives (Guo et al. 2019). Recent transcriptomic studies in ferns have identified widespread duplications of cell wall biosynthesis genes (Ali et al. 2025). Consistent with these patterns, arborescent Cyatheaceae species retained ohnologs enriched in cell wall biosynthesis pathways, presumably underpinning the evolution of their trunk-like stems, whereas nonarborescent species preferentially preserved ohnologs linked to metabolic and defensive pathways that support drought tolerance and herbivore resistance. Unlike the aquatic fern *Ceratopteris richardii*, which rapidly purged most WGD-derived genes following polyploidy (Marchant et al. 2022), tree ferns retained and repurposed these ancient gene duplicates into a dual-phase evolutionary reservoir, serving both as a buffer against immediate environmental upheavals and as a source of genomic material for long-term niche diversification and phenotypic novelties. However, gene copy accumulation alone was not sufficient for morphological innovation and ecological adaptation. The realization of arborescent adaptations required precise coordination of duplicate gene expression and regulation, as we discuss next.

Regulatory Innovation Over Gene Dosage Underpinning Arborescence

The functional dichotomy between arborescent and nonarborescent tree ferns arises from regulatory innovation rather than simple gene dosage effects. Our comparative analyses highlight transcriptional reprogramming as essential for converting genomic potential derived from WGD into the distinct growth forms observed. For example, the nonarborescent *G. denticulata* exhibits fewer copies of key polymerization enzymes (e.g. *POX/LAC*) than its arborescent relatives, although it retains a higher number of some lignin biosynthesis genes (*CesA/Csl*). Crucially, *G. denticulata* shows significantly reduced expression of both *POX/LAC* and *CesA/Csl* genes. This imbalance indicates that despite retaining certain cellulose-related genes, *G. denticulata* has a limited capacity for lignin deposition, mirroring lignin-reduction strategies observed in aquatic plants (Ma et al. 2024). Arborescent lineages not only exhibit upregulation of WGD-derived *POX/LAC* and *CesA* genes in stems but also show expanded copy numbers of *CRY* photoreceptors and *NAC* transcription factors, which are central to blue light–mediated secondary wall thickening (Zhang et al. 2018). These findings suggest that arborescent lineages did not merely inherit the genomic substrates for arborescence, but actively evolved the regulatory architecture necessary to mobilize them in building trunk-like stems. In particular, our data suggest a possible dual role for *CRY*-mediated signaling in tree ferns, promoting lignification while concurrently enhancing shade tolerance, which mirrors the mechanism observed in *Arabidopsis* (Zhang et al. 2018). In parallel, the expansion of *CRY* genes may have facilitated adaptation to low-light understory environments dominated by angiosperms, as previously reported in leptosporangiate ferns (Cai et al. 2021). These genomic changes align with macroevolutionary evidence that the rise of angiosperms created novel ecological niches, promoting diversification among shade-dwelling ferns (Wu et al. 2025). In addition to the upregulation of lignin biosynthetic components, recent work shows that *bHLH* transcription factors are co-expressed with these pathway elements in tree ferns (Huang et al. 2025), further underscoring the regulatory complexity underlying arborescence. In contrast, nonarborescent species elevate the expression of defense-related paralogs, reflecting an adaptive trade-off that favors metabolic resilience and stress tolerance over structural reinforcement. Given the complexity of this coordinated regulatory framework, future functional studies are needed to elucidate how these candidate genes contribute to shade tolerance and lignification in tree ferns. Although genetic transformation in tree ferns remains challenging, emerging gene-editing platforms in model ferns such as *Ceratopteris richardii* (Jiang et al. 2024; Xiang and Li 2024) may offer promising avenues for the functional validation of these key genes. Collectively, our findings underscore that the evolutionary innovation of arborescence in tree ferns was likely shaped by dynamic transcriptional reprogramming of duplicate genes rather than by passive gene retention alone.

TE-Mediated Innovation Amid Syntenic Conservation

Tree fern genomes exhibit cryptic dynamism through TE-mediated diversification despite conserved macrosynteny. As dominant repeat elements in plant genomes (Hawkins et al. 2006), LTR-RTs have proliferated variably across tree fern species. Solo-LTRs are indicative of genomic purging and downsizing, which can be formed by the unequal recombination (Cossu et al. 2017). The ratio of solo-LTRs to intact-LTRs serves as a key indicator for estimating the extent of recombination and the efficiency of LTR element removal through deletion (Jedlicka et al. 2020). Genome reduction in *S. brunoniana* appears to be driven by efficient DNA removal mechanisms, as supported by the reduced cumulative length of intact-LTR retrotransposons (including Ty3/*Gypsy* and Ty1/*Copia*) and a high solo-LTR to intact-LTR ratio. In contrast, species such as *S. lepifera* and *G. denticulata* show substantial expansion of LTR-RTs, which strongly correlate with their expanded intergenic regions and larger genome size. This pattern aligns with observations in other seed-free vascular plants, where TE activity—particularly that of LTR-RTs—drives genome size evolution independently of polyploidy (Bennetzen et al. 2005; Vitte and Panaud 2005; Niu et al. 2019). The variation in solo-/intact-LTR ratios across species indicates differential LTR turnover rates, highlighting the highly dynamic evolutionary trajectory of tree fern genomes. This genomic dynamism is further evidenced by the widespread prevalence of highly polymorphic LTR-RTs across plant species (Morales-Díaz et al. 2025), reinforcing their role as a fundamental driver of structural variation and genome diversification. While TE insertions can disrupt gene function when inserted into coding or regulatory regions, they more often act as engines of evolutionary innovation (Galindo-González et al. 2017; Catoni 2024). Transposons provide raw genetic material for adaptation through lineage-specific chromosomal rearrangements and functional diversification. Despite the global syntenic conservation, TE-enriched regions in tree ferns have emerged as localized hotspots of rapid evolution. These regions exhibit notable genomic dynamism, including elevated substitution rates and rewired transcriptional networks. This

mirrors evolutionary patterns in the living fossil gymnosperms *Ginkgo* (Liu et al. 2021) and *Cycas* (Liu et al. 2022), where TEs drive localized adaptive hotspots while preserving ancestral morphologies. Such duality—global stability paired with localized plasticity—suggests a mechanism reconciling how morphologically static ferns have persisted through environmental upheavals, positioning TEs as genomic "pressure valves" that enable attuned adaptation without compromising global genome stability.

Integration and Evolutionary Implications: Reconciling Stasis With Dynamism

Our study resolves the long-standing stasis-dynamism paradox by demonstrating that tree ferns achieve evolutionary persistence through a regulated form of genomic dynamism—a balanced system in which ultralow genome-wide substitution rates coexist with bursts of innovation in specific genomic regions. Our analysis of absolute substitution rates confirms that Cyatheaceae genomes evolve at an exceptionally slow pace—~3-fold slower than those of other ferns. This extreme genomic deceleration may partly explain the relatively low species diversity in Cyatheaceae when compared with the highly diverse families such as Polypodiaceae (PPG I 2016). Previous studies often interpreted the ultralow molecular substitution rates observed in "living fossil" lineages as a proxy for genomic stasis, assuming that a slow rate of DNA change constrains the evolutionary flexibility in ancient lineages with long-term morphological stasis (Bomfleur et al. 2014; Schneider et al. 2015; Clark et al. 2016; Brownstein et al. 2024). However, many of these studies were limited to karyotypic comparisons, sparse loci sampling, or a single reference genome, and therefore failed to capture lineage-specific genomic dynamics. In contrast, our integrated approach employing multiple chromosome-scale genomes and comparative transcriptomic data across diverse Cyatheaceae species revealed pan-lineage evolutionary mechanisms, such as diversification of stress responses and niche specialization, albeit with overall slow molecular evolutionary rates.

Crucially, we show that low substitution rates and considerable genomic plasticity coexist in Cyatheaceae through synergistic processes acting in concert: the repurposing of WGD-derived paralogs for new functions, TE-driven genome restructuring that creates localized adaptive innovations, and the recalibration of regulatory frameworks to facilitate phenotypic novelty. These mechanisms align with certain evolutionary strategies observed in other long-persisting lineages. For example, the living fossil gymnosperms like Ginkgo and cycads also exhibit combinations of ancient genome duplications and TE accumulations coupled with constrained morphological change (Liu et al. 2021, 2022). Indeed, dynamic genomic evolution, such as ancient polyploidy and TE bursts, has been increasingly documented even in ferns (Huang et al. 2022; Marchant et al. 2022; Fernández et al. 2024). This growing evidence from distantly related lineages suggests that evolutionary stasis can be an active process sustained by repurposing genomic elements under regulatory constraints, rather than a passive genomic stagnation without genomic change. Collectively, our findings redefine evolutionary stasis in ancient fern lineages as a dynamic equilibrium. This equilibrium functions as a slow-release evolutionary strategy, balancing cryptic genomic innovation with morphological conservatism, enabling their persistence through deep time.

Conclusions

Our study demonstrates that the evolutionary stasis-dynamism paradox in tree ferns reflects a dynamic genomic equilibrium rather than passive consequence of genomic stagnation, wherein profound morphological conservation coexists with substantial genomic change. A shared Jurassic WGD event across Cyatheaceae likely buffered past environmental upheavals while providing long-term raw materials for adaptive innovation. Recurrent TE activity promoted structural diversity and genome size variation, precipitating localized hotspots of accelerated sequence turnover. In parallel, coordinated regulatory recalibrations, as well as the putative co-option of a light-responsive module for both shade adaptation and lignification, may have facilitated tree ferns' persistence in angiosperm-dominated understories. Our findings have broad implications in that ancient "living fossil" lineages can persist across geological timescales by balancing ultralow rates of neutral evolution with attuned genomic innovation, illustrating that morphological stasis does not imply evolutionary stagnation but rather conceals a latent dynamism enabling long-term survival. Future comparative studies that integrate genomic, epigenomic, and functional data across diverse persisting lineages will further advance our understanding of how genome dynamics sustain evolutionary longevity.

Materials and Methods

Genome Assembly

Fresh leaves of *S. brunoniana*, *G. denticulata*, and *S. lepifera* were collected from South China National Botanical Garden, Nankunshan National Forest Park (Guangdong, China), and Shanghai Chenshan Botanical Garden (Shanghai, China), respectively. High-quality genomic DNA was extracted using a cetyltrimethylammonium bromide protocol (Winnepenninckx et al. 1993). For *S. brunoniana* and *G. denticulata*, PacBio HiFi long reads were assembled with hifiasm (v0.16.1-r37526) (Cheng et al. 2021) under default parameters, followed by misjoin correction and scaffolding with Juicer (v1.6) (Durand et al. 2016) and 3D-DNA (v201008) (Dudchenko et al. 2017). An existing draft genome of *S. lepifera* was enhanced similarly using Juicer and 3D-DNA to obtain chromosome-level scaffolds. The completeness of each final genome assembly was assessed with BUSCO (v5.2.2) (Simão et al. 2015) using the eukaryota_odb10 (Kriventseva et al. 2019). Additional details, including sequencing coverage and assembly statistics, are described in supplementary Note 1 and Table S1.

Genome Annotation

Repeat sequences were identified by a combination of de novo and homology-based approaches. A de novo repeat library was first constructed using RepeatModeler (v2.0.1) (Flynn et al. 2020) and LTR_FINDER (v1.0.6) (Xu and Wang 2007). Both RepeatMasker (v.4.1.0) (Tarailo-Graovac and Chen 2009) with parameters -nolow -no_is -norna and RepeatProteinMask (v.4.0.7) (Tarailo-Graovac and Chen 2009) with parameters -noLowSimple *P*-value 0.0001 were then applied to perform a homology-based repeat search leveraging the de novo repeat database and Repbase (Jurka et al. 2005). Overlapping repeats from the same class were merged

based on genomic coordinates. In addition, we also used the pipeline from LTR_retriever (Ou and Jiang 2018) to identify all LTR retrotransposons and isolate solo-LTRs using the dedicated scripts provided in the LTR_retriever.

Protein-coding genes (CDSs) were predicted by integrating evidence from three independent approaches: RNA-seq evidence, ab initio prediction, and protein homology. For RNA-seq data, reads from leaves, roots, and stems were aligned to each genome using HISAT2 (v2.1.0) (Kim et al. 2015), followed by transcript assembly with Stringtie (v1.2.3) (Pertea et al. 2015) to obtain transcript-based annotation. CDSs were predicted using Transdecoder (https://github.com/TransDecoder). Trinity (v2.15.0) (Grabherr et al. 2011) was used to de novo assemble the transcriptome and PASA (https://github.com/PASApipeline/PASApipeline) was further used to update the assembly. Ab initio predictions were conducted using AUGUSTUS (Stanke and Morgenstern 2005) and GlimmerHMM (Majoros et al. 2004) with default parameters. For homology-based annotation, protein sequences from six reference species (*C. richardii*, *A. spinulosa*, *Adiantum capillus-veneris*, *Azolla filiculoides*, *Marsilea vestita*, and *Selaginella moellendorffii*) were aligned against the assembled genomes with TBLASTN searches against the assemblies (*E*-value $\leq 1 \times 10^{-5}$), followed by transcript generation using Exonerate. The results from these three approaches were integrated into a nonredundant gene model set using MAKER (v.2.31.10) (Holt and Yandell 2011). Gene functional annotation was performed by searching multiple public protein databases including Nr, Uniprot, KOG, InterPro, Pfam, GO and KEGG databases.

Identification and Dating of WGD Events

We used an integrated approach combining the synteny, K_S age distribution and gene tree-species tree reconciliation-based phylogenomic methods to detect and date WGDs. First, we performed all-against-all BLASTP (*E*-value $<10^{-10}$) within and between genomes using MCScanX (Wang et al. 2012) to identify intra- and interspecific syntenic blocks. Dot plots and syntenic depth ratios were visualized with JCVI (Tang et al. 2008), while the WGDI toolkit (Sun et al. 2022) was used to annotate syntenic gene pairs with K_S values.

Next, K_S-based age distributions were generated for the whole paranome and for anchor pairs using wgd v2 (Chen et al. 2024). We applied "wgd dmd" to construct the whole paranome and "wgd syn" to detect synteny with i-ADHoRe (v3.0.01) (Proost et al. 2012) and "wgd ksd" to calculate K_S values. ELMMs and log-scale GMMs were then used to delineate WGD peaks. Based on the paralogous K_S distribution, we then selected species *G. denticulata*, *S. lepifera*, *S. brunoniana*, *Dicksonia antarctica*, *Cibotium barometz*, *Thyrsopteris elegans*, *Plagiogyria japonica*, *Culcita macrocarpa*, *M. vestita*, *M. quadrifolia*, two outgroups *Lygodium japonicum* and *L. flexuosum*, to construct orthologous K_S distributions in order to delineate the phylogenetic location of the WGD event with substitution rate correction (Fig. S21), following the instructed pipeline in wgd v2 (Chen et al. 2024).

For phylogenomic reconciliation, we utilized the software WHALE (v.2.0.3) (Zwaenepoel and Van de Peer 2019). Gene families were built via OrthoFinder (v2.3.3) (Emms and Kelly 2015), filtering out families that are excessively large or lack genes from both branches at the root with orthofilter.py (https://github.com/arzwa/Whale.jl). Multiple sequence alignments were produced by PRANK (v150803) (Löytynoja and Goldman 2005), and posterior distributions of gene trees were inferred using Mrbayes (v3.2.6) (Ronquist et al. 2012) under the LG + GAMMA model. We used ALEobserve (Szöllősi et al. 2013) to construct the conditional clade distributions, which were incorporated into WHALE under critical and relaxed branch-specific DL + WGD models to test alternative scenarios of WGD events with parameters following Chen et al. (2022).

Finally, absolute dating of the WGD events followed the pipeline of wgd v2 (Chen et al. 2024), calibrated with a starting tree topology and fossil constraints (Fig. S22 and Table S17). Details of the species, data types, and data sources used in these analyses are provided in Table S18.

Identification and Functional Enrichment of Retained Genes Following WGD

To explore the functional significance of gene duplicates retained from the inferred WGD, we classified duplicate pairs into two groups: commonly retained (present in all four Cyatheaceae species) or biasedly retained (found in only one lineage). First, we identified species-specific gene families using OrthoFinder outputs. Within each genome, anchor genes in inter- and intragenomic synteny blocks were identified. Anchor genes present in intergenomic blocks but exclusively found in intragenomic blocks of a single species were labeled as biasedly retained. In contrast, anchor genes shared across the four Cyatheaceae species were defined as commonly retained. GO enrichment analysis of the retained genes following WGD was performed using the R package clusterProfiler (Wu et al. 2021), and the results were visualized with circos plots generated by Circos (Krzywinski et al. 2009).

Phylogenetic Inference and Gene Family Analysis

Gene families (i.e. orthogroups) were constructed from proteomes of 15 representative species (Table S19) using OrthoFinder (v2.5.4) (Emms and Kelly 2015) with an inflation factor of 2.0. We retained 143 single-copy orthogroups present in at least 70% of the species for phylogenetic tree construction. Each orthogroup was aligned using MAFFT (v7.505) (Katoh and Standley 2013) and subsequently trimmed with trimAl (v1.4.rev15) (Capella-Gutiérrez et al. 2009). The resulting alignments were concatenated into a supergene matrix and used to construct a maximum-likelihood phylogenetic tree with IQ-TREE2 (v2.2.0.3) (Minh et al. 2020), employing 1,000 bootstrap replicates. Divergence times were subsequently estimated via MCMCtree integrated within PAML (v4.9i) (Yang 2007) with the following constraints: (i) 125 to 251 Ma for Cyatheaceae (Lehtonen et al. 2017); (ii) 330.9 to 365 Ma for seed plants (Morris et al. 2018); (iii) > 420 Ma for lycophytes (Testo et al. 2018); and (iv) 472 to 444 Ma for land plant (Testo et al. 2018). Gene family expansion and contraction were inferred using CAFÉ (v5.1) (Mendes et al. 2021) at a significance level of $P < 0.05$. Gene family clustering was performed on the online web server OrthoVenn3 (Sun et al. 2023), with protein sequences of seven ferns as inputs.

For additional gene family analysis derived from reference orthologs, we combined HMMER and BLASTP to identify gene family members. Briefly, known genes from *Arabidopsis thaliana* and *Populus trichocarpa* were used as queries (Table S20) to perform BLASTP searches against the proteomes of *S. lepifera*, *S. brunoniana*, *A. spinulosa*, and *G. denticulata*. BLAST hits with identity >40% and *E*-value <1e−10 were retained. Besides, the hidden Markov model

(HMM) of gene families from the Pfam protein family database was used to search genes in each species using HMMER (v 3.1b2) (Eddy 2011) with default parameters. The homologous sequences of Cyatheaceae were then obtained by combining both results above. We further filtered homologous sequences based on their conserved protein domains using the Pfam, SMART, and NCBI Conserved Domains databases. Multiple sequence alignment was constructed with MAFFT (v7.505) (Katoh and Standley 2013) using default parameters, followed by phylogenetic inference with IQ-TREE2 (v2.2.0.3) (Minh et al. 2020). For identification of lignin genes, we used the known genes in the lignin biosynthesis pathway from *A. spinulosa* and *Ar. thaliana* as seed sequences to identify their homologs in the other three Cyatheaceae species at an *E*-value cutoff of 1e−10.

Evolutionary Rate Estimation and Synteny Retention

We evaluated substitution rates using 583 low-copy orthogroups (one or two genes per species) selected from the 15 species OrthoFinder dataset. Multiple sequence alignments for each orthogroup were analyzed using CODEML module in PAML (v4.9i) (Yang 2007) under both free-ratio and one-ratio models, yielding lineage-specific d_N and d_S. Evolutionary rate rankings were determined through multiple comparison analyses in SPSS. Absolute molecular evolutionary rates for each species were inferred using the penalized likelihood method in r8s (v1.8) (Sanderson 2003).

To investigate synteny loss variation, we performed genome alignments of seven chromosome-level fern assemblies against five outgroups (*Diphasiastrum complanatum*, *Ginkgo biloba*, *Amborella trichopoda*, *Aristolochia fimbriata*, and *Acorus tatarinowii*) using JCVI (Tang et al. 2008). Syntenic block sizes were quantified based on the number of anchor gene pairs, whereas the relative syntenic retention rates reflected the proportion of each outgroup's genes found in collinear segments with the fern genomes.

Genomic Synteny Analyses and Detection of Rearrangements

To detect genomic synteny and potential rearrangements among the four Cyatheaceae species, we initially employed JCVI (Tang et al. 2008) to search for syntenic blocks by comparing the three newly assembled genomes to the *A. spinulosa* reference. Collinear blocks were filtered to retain one-to-one best hits (–cscore = 0.99) with a minimum span of 30 genes (–minspan = 30) for downstream analysis and visualization. Lineage-specific fusion events in *G. denticulata* were further examined using D-GENIES (Cabanettes and Klopp 2018) to generate detailed synteny maps. To further assess whether TE activity underlies these breakpoints, we compared TE density in the 20-Mb regions flanking each breakpoint with TE densities in 10,000 randomly sampled regions of equivalent length from the same chromosome. A Wilcoxon signed-rank test was then conducted to determine whether flanking regions of identified breakpoints had significantly greater TE content than the genomic background.

Transcriptome Analyses

Total RNA was extracted from four tissues (root, frond, stem, and stipe) of the three arborescent Cyatheaceae species, and from three tissues (root, frond, and stem) of the nonarborescent *G. denticulata*, each with three biological replicates. Raw reads were trimmed by Fastp (v0.23.2) (Chen et al. 2018) and aligned to the genomes using HISAT2 (v2.1.0) (Kim et al. 2015) under default settings. Gene expression levels were quantified as fragment counts using FeatureCounts (v2.0.3) (Liao et al. 2014), and genes with FPKM >1 were considered expressed.

Supplementary material

Supplementary material is available at *Molecular Biology and Evolution* online.

Acknowledgments

J.W. and M.K. acknowledge funding from the Guangdong S&T Program (2022B1111230001), the National Natural Science Foundation of China (32170382, 32370404), the Natural Science Foundation of Guangdong Province (2022A1515011293), and the Guangdong Flagship Project of Basic and Applied Basic Research (2023B0303050001). Z.W. acknowledges funding from the China Scholarship Council (No. 202304910357). The authors thank Y.H. Yan for sharing raw genome sequencing data of *S. lepifera*, and the Shanghai Chenshan Botanical Garden for providing the plant material of *S. lepifera* for Hi-C sequencing. The authors appreciate Dr S.Y. Dong's help with species identification. They thank J.Y. Xu, Q. Yuan, S.G. Li, and Q.M. Lu for their assistance with sample collection, X. Ma for her help with the comparative genome analysis, S. Rombauts for his help with uploading the new genome assemblies and annotations, and F. Almeida-Silva for his help with R scripts for figure visualization.

Author Contributions

J.W. and M.K.: Conceptualization. Z.W.: Formal analyses, Writing—original draft. H.C.: Methodology, Validation. Z.X.: Methodology. C.F.: Methodology. J.W., M.K., and Y.V.d.P.: Writing—review & editing. All authors read and approved the final manuscript.

Competing Interests

The authors declare no competing interests.

Data Availability

All sequencing data have been deposited at NCBI under the BioProject accession number PRJNA1234874. Genome assemblies with annotations are available at ORCAE (https://bioinformatics.psb.ugent.be/orcae/overview/Gymde, https://bioinformatics.psb.ugent.be/orcae/overview/Sphbr, and https://bioinformatics.psb.ugent.be/orcae/overview/Sphle).

References

Ali Z *et al.* Comparative transcriptomics in ferns reveals key innovations and divergent evolution of the secondary cell walls. *Nat Plants*. 2025:11:1028–1048. https://doi.org/10.1038/s41477-025-01978-y.

Bennetzen JL, Ma J, Devos KM. Mechanisms of recent genome size variation in flowering plants. *Ann Bot*. 2005:95:127–132. https://doi.org/10.1093/aob/mci008.

Bomfleur B, Mcloughlin S, Vajda V. Fossilized nuclei and chromosomes reveal 180 million years of genomic stasis in royal ferns. *Science*. 2014:343:1376–1377. https://doi.org/10.1126/science.1249884.

Brownstein CD *et al.* The genomic signatures of evolutionary stasis. *Evolution*. 2024:78:821–834. https://doi.org/10.1093/evolut/qpae028.
Cabanettes F, Klopp C. D-GENIES: dot plot large genomes in an interactive, efficient and simple way. *PeerJ*. 2018:6:e4958. https://doi.org/10.7717/peerj.4958.
Cai S *et al.* Evolution of rapid blue-light response linked to explosive diversification of ferns in angiosperm forests. *New Phytol*. 2021:230:1201–1213. https://doi.org/10.1111/nph.17135.
Capella-Gutiérrez S, Silla-Martínez JM, Gabaldón T. Trimal: a tool for automated alignment trimming in large-scale phylogenetic analyses. *Bioinformatics*. 2009:25:1972–1973. https://doi.org/10.1093/bioinformatics/btp348.
Catoni M. Transposable elements underlie genetic adaptation. *Nat Plants*. 2024:10:1617–1618. https://doi.org/10.1038/s41477-024-01792-y.
Chen H *et al.* Revisiting ancient polyploidy in leptosporangiate ferns. *New Phytol*. 2022:237:1405–1417. https://doi.org/10.1111/nph.18607.
Chen H, Zwaenepoel A, Van de Peer Y. wgd v2: a suite of tools to uncover and date ancient polyploidy and whole-genome duplication. *Bioinformatics*. 2024:40:btae272. https://doi.org/10.1093/bioinformatics/btae272.
Chen S, Zhou Y, Chen Y, Gu J. fastp: an ultra-fast all-in-one FASTQ preprocessor. *Bioinformatics*. 2018:34:i884–i890. https://doi.org/10.1093/bioinformatics/bty560.
Chen ZJ *et al.* Genomic diversifications of five *Gossypium* allopolyploid species and their impact on cotton improvement. *Nat Genet*. 2020:52:525–533. https://doi.org/10.1038/s41588-020-0614-5.
Cheng H, Concepcion GT, Feng X, Zhang H HL. Haplotype-resolved de novo assembly using phased assembly graphs with hifiasm. *Nat Methods*. 2021:18:170–175. https://doi.org/10.1038/s41592-020-01056-5.
Chomicki G, Coiro M, Renner SS. Evolution and ecology of plant architecture: integrating insights from the fossil record, extant morphology, developmental genetics and phylogenies. *Ann Bot*. 2017:120:855–891. https://doi.org/10.1093/aob/mcx113.
Clark J *et al.* Genome evolution of ferns: evidence for relative stasis of genome size across the fern phylogeny. *New Phytol*. 2016:210:1072–1082. https://doi.org/10.1111/nph.13833.
Clark JW. Genome evolution in plants and the origins of innovation. *New Phytol*. 2023:240:2204–2209. https://doi.org/10.1111/nph.19242.
Cossu RM *et al.* LTR retrotransposons show low levels of unequal recombination and high rates of intraelement gene conversion in large plant genomes. *Genome Biol Evol*. 2017:9:3449–3462. https://doi.org/10.1093/gbe/evx260.
Dudchenko O *et al.* De novo assembly of the *Aedes aegypti* genome using Hi-C yields chromosome-length scaffolds. *Science*. 2017:356:92–95. https://doi.org/10.1126/science.aal3327.
Durand NC *et al.* Juicer provides a one-click system for analyzing loop-resolution hi-C experiments. *Cell Syst*. 2016:3:95–98. https://doi.org/10.1016/j.cels.2016.07.002.
Eddy SR. Accelerated profile HMM searches. *PLoS Comput Biol*. 2011:7:e1002195. https://doi.org/10.1371/journal.pcbi.1002195.
Emms DM, Kelly S. OrthoFinder: solving fundamental biases in whole genome comparisons dramatically improves orthogroup inference accuracy. *Genome Biol*. 2015:16:157. https://doi.org/10.1186/s13059-015-0721-2.
Fang Y *et al.* The genome of homosporous maidenhair fern sheds light on the euphyllophyte evolution and defences. *Nat Plants*. 2022:8:1024–1037. https://doi.org/10.1038/s41477-022-01222-x.
Fernández P *et al.* Giant fern genomes show complex evolution patterns: a comparative analysis in two Species of *Tmesipteris* (Psilotaceae). *Int J Mol Sci*. 2023:24:2708. https://doi.org/10.3390/ijms24032708.
Fernández P *et al.* A 160 Gbp fork fern genome shatters size record for eukaryotes. *iScience*. 2024:27:109889. https://doi.org/10.1016/j.isci.2024.109889.
Flynn JM *et al.* RepeatModeler2 for automated genomic discovery of transposable element families. *Proc Natl Acad Sci U S A*. 2020:117:9451–9457. https://doi.org/10.1073/pnas.1921046117.
Fujiwara T *et al.* Evolution of genome space occupation in ferns: linking genome diversity and species richness. *Ann Bot*. 2023:131:59–70. https://doi.org/10.1093/aob/mcab094.
Galindo-González L, Mhiri C, Deyholos MK, Grandbastien MA. LTR-retrotransposons in plants: engines of evolution. *Gene*. 2017:626:14–25. https://doi.org/10.1016/j.gene.2017.04.051.
Gommers CM, Visser EJ, St Onge KR, Voesenek LA, Pierik R. Shade tolerance: when growing tall is not an option. *Trends Plant Sci*. 2013:18:65–71. https://doi.org/10.1016/j.tplants.2012.09.008.
Grabherr MG *et al.* Full-length transcriptome assembly from RNA-Seq data without a reference genome. *Nat Biotechnol*. 2011:29:644–652. https://doi.org/10.1038/nbt.1883.
Guo ZH *et al.* Genome sequences provide insights into the reticulate origin and unique traits of woody bamboos. *Mol Plant*. 2019:12:1353–1365. https://doi.org/10.1016/j.molp.2019.05.009.
Haufler CH. Ever since Klekowski: testing a set of radical hypotheses revives the genetics of ferns and lycophytes. *Am J Bot*. 2014:101:2036–2042. https://doi.org/10.3732/ajb.1400317.
Hawkins JS, Kim H, Nason JD, Wing RA, Wendel JF. Differential lineage-specific amplification of transposable elements is responsible for genome size variation in *Gossypium*. *Genome Res*. 2006:16:1252–1261. https://doi.org/10.1101/gr.5282906.
Holt C, Yandell M. MAKER2: an annotation pipeline and genome-database management tool for second-generation genome projects. *BMC Bioinformatics*. 2011:12:491. https://doi.org/10.1186/1471-2105-12-491.
Huang CH, Qi X, Chen D, Qi J, Ma H. Recurrent genome duplication events likely contributed to both the ancient and recent rise of ferns. *J Integr Plant Biol*. 2020:62:433–455. https://doi.org/10.1111/jipb.12877.
Huang X *et al.* The flying spider-monkey tree fern genome provides insights into fern evolution and arborescence. *Nat Plants*. 2022:8:500–512. https://doi.org/10.1038/s41477-022-01146-6.
Huang X *et al.* Genome-wide identification of five fern bHLH families and functional analysis of bHLHs in lignin biosynthesis in *Alsophila spinulosa*. *BMC Genomics*. 2025:26:357. https://doi.org/10.1186/s12864-025-11522-z.
Jedlicka P, Lexa M, Kejnovsky E. What can long terminal repeats tell us about the age of LTR retrotransposons, gene conversion and ectopic recombination? *Front Plant Sci*. 2020:11:644. https://doi.org/10.3389/fpls.2020.00644.
Jiang W *et al.* Efficient gene editing of a model fern species through gametophyte-based transformation. *Plant Physiol*. 2024:196:2346–2361. https://doi.org/10.1093/plphys/kiae473.
Judd EJ *et al.* A 485-million-year history of Earth's surface temperature. *Science*. 2024:385:eadk3705. https://doi.org/10.1126/science.adk3705.
Jurka J *et al.* Repbase update, a database of eukaryotic repetitive elements. *Cytogenet Genome Res*. 2005:110:462–467. https://doi.org/10.1159/000084979.
Katayama N, Yamamoto T, Aiuchi S, Watano Y, Fujiwara T. Subgenome evolutionary dynamics in allotetraploid ferns: insights from the gene expression patterns in the allotetraploid species *Phegopteris decursivepinnata* (Thelypteridacea, Polypodiales). *Front Plant Sci*. 2024:14:1286320. https://doi.org/10.3389/fpls.2023.1286320.
Katoh K, Standley DM. MAFFT multiple sequence alignment software version 7: improvements in performance and usability. *Mol Biol Evol*. 2013:30:772–780. https://doi.org/10.1093/molbev/mst010.
Kenrick P, Crane P. The origin and early evolution of plants on land. *Nature*. 1997:389:33–39. https://doi.org/10.1038/37918.
Khandelwal S. Chromosome evolution in the genus *Ophioglossum* L. *Bot J Linn Soc*. 1990:102:205–217. https://doi.org/10.1111/j.1095-8339.1990.tb01876.x.
Kim D, Langmead B, Salzberg SL. HISAT: a fast spliced aligner with low memory requirements. *Nat Methods*. 2015:12:357–360. https://doi.org/10.1038/nmeth.3317.

Klekowski EJ, Baker HG. Evolutionary significance of polyploidy in the Pteridophyta. *Science*. 1966:153:305–307. https://doi.org/10.1126/science.153.3733.305.

Korall P, Schuettpelz E, Pryer KM. Abrupt deceleration of molecular evolution linked to the origin of arborescence in ferns. *Evolution*. 2010:64:2786–2792. https://doi.org/10.1111/j.1558-5646.2010.01000.x.

Kriventseva EV *et al.* OrthoDB v10: sampling the diversity of animal, plant, fungal, protist, bacterial and viral genomes for evolutionary and functional annotations of orthologs. *Nucleic Acids Res*. 2019:47:D807–D811. https://doi.org/10.1093/nar/gky1053.

Krzywinski M *et al.* Circos: an information aesthetic for comparative genomics. *Genome Res*. 2009:19:1639–1645. https://doi.org/10.1101/gr.092759.109.

Lehtonen S *et al.* Environmentally driven extinction and opportunistic origination explain fern diversification patterns. *Sci Rep*. 2017:7:4831. https://doi.org/10.1038/s41598-017-05263-7.

Liao Y, Smyth GK, Shi W. featureCounts: an efficient general purpose program for assigning sequence reads to genomic features. *Bioinformatics*. 2014:30:923–930. https://doi.org/10.1093/bioinformatics/btt656.

Liu H *et al.* The nearly complete genome of *Ginkgo biloba* illuminates gymnosperm evolution. *Nat Plants*. 2021:7:748–756. https://doi.org/10.1038/s41477-021-00933-x.

Liu Y *et al.* The *Cycas* genome and the early evolution of seed plants. *Nat Plants*. 2022:8:389–401. https://doi.org/10.1038/s41477-022-01129-7.

Loiseau O *et al.* Slowly but surely: gradual diversification and phenotypic evolution in the hyper-diverse tree fern family Cyatheaceae. *Ann Bot*. 2020:125:93–103. https://doi.org/10.1093/aob/mcz145.

Long W *et al.* Genome evolution and diversity of wild and cultivated rice species. *Nat Commun*. 2024:15:9994. https://doi.org/10.1038/s41467-024-54427-3.

Löytynoja A, Goldman N. An algorithm for progressive multiple alignment of sequences with insertions. *Proc Natl Acad Sci U S A*. 2005:102:10557–10562. https://doi.org/10.1073/pnas.0409137102.

Ma X *et al.* Seagrass genomes reveal ancient polyploidy and adaptations to the marine environment. *Nat Plants*. 2024:10:240–255. https://doi.org/10.1038/s41477-023-01608-5.

Majoros WH, Pertea M, Salzberg SL. TigrScan and GlimmerHMM: two open source ab initio eukaryotic gene-finders. *Bioinformatics*. 2004:20:2878–2879. https://doi.org/10.1093/bioinformatics/bth315.

Marchant DB *et al.* Dynamic genome evolution in a model fern. *Nat Plants*. 2022:8:1038–1051. https://doi.org/10.1038/s41477-022-01226-7.

McCahill IW, Hazen SP. Regulation of cell wall thickening by a medley of mechanisms. *Trends Plant Sci*. 2019:24:853–866. https://doi.org/10.1016/j.tplants.2019.05.012.

Mendes FK, Vanderpool D, Fulton B MWH. CAFE 5 models variation in evolutionary rates among gene families. *Bioinformatics*. 2021:36:5516–5518. https://doi.org/10.1093/bioinformatics/btaa1022.

Minh BQ *et al.* IQ-TREE 2: new models and efficient methods for phylogenetic inference in the genomic era. *Mol Biol Evol*. 2020:37:1530–1534. https://doi.org/10.1093/molbev/msaa015.

Morales-Díaz N *et al.* Tandem LTR-retrotransposon structures are common and highly polymorphic in plant genomes. *Mob DNA*. 2025:16:10. https://doi.org/10.1186/s13100-025-00347-y.

Morris JL *et al.* The timescale of early land plant evolution. *Proc Natl Acad Sci U S A*. 2018:115:E2274–E2283. https://doi.org/10.1073/pnas.1719588115.

Nakato N. Cytological studies on the genus *Cyathea* in Japan. *J Jpn Bot*. 1989:64:142–147. https://doi.org/10.51033/jjapbot.64_5_8317.

Niklas K, Tiffney B, Knoll A. Patterns in vascular land plant diversification. *Nature*. 1983:303:614–616. https://doi.org/10.1038/303614a0.

Niu XM *et al.* Transposable elements drive rapid phenotypic variation in *Capsella rubella*. *Proc Natl Acad Sci U S A*. 2019:116:6908–6913. https://doi.org/10.1073/pnas.1811498116.

Ou S, Jiang N. LTR_retriever: a highly accurate and sensitive program for identification of long terminal repeat retrotransposons. *Plant Physiol*. 2018:176:1410–1422. https://doi.org/10.1104/pp.17.01310.

Pelosi JA, Kim EH, Barbazuk WB, Sessa EB. Phylotranscriptomics illuminates the placement of whole genome duplications and gene retention in ferns. *Front Plant Sci*. 2022:13:882441. https://doi.org/10.3389/fpls.2022.882441.

Pertea M *et al.* StringTie enables improved reconstruction of a transcriptome from RNA-seq reads. *Nat Biotechnol*. 2015:33:290–295. https://doi.org/10.1038/nbt.3122.

PPG I. A community-derived classification for extant lycophytes and ferns. *J Syst Evol*. 2016:54:563–603. https://doi.org/10.1111/jse.12229.

Proost S *et al.* i-ADHoRe 3.0-fast and sensitive detection of genomic homology in extremely large data sets. *Nucleic Acids Res*. 2012:40:e11. https://doi.org/10.1093/nar/gkr955.

Pryer KM *et al.* Phylogeny and evolution of ferns (monilophytes) with a focus on the early leptosporangiate divergences. *Am J Bot*. 2004:91:1582–1598. https://doi.org/10.3732/ajb.91.10.1582.

Qin G *et al.* Chromosome-scale genome of the fern *Cibotium barometz* unveils a genetic resource of medicinal value. *Horticulturae*. 2024:10:1191. https://doi.org/10.3390/horticulturae10111191.

Rahmatpour N *et al.* Analyses of *Marsilea vestita* genome and transcriptomes do not support widespread intron retention during spermatogenesis. *New Phytol*. 2023:237:1490–1494. https://doi.org/10.1111/nph.18652.

Rice A *et al.* The Chromosome Counts Database (CCDB)—a community resource of plant chromosome numbers. *New Phytol*. 2015:206:19–26. https://doi.org/10.1111/nph.13191.

Ronquist F *et al.* Mrbayes 3.2: efficient Bayesian phylogenetic inference and model choice across a large model space. *Syst Biol*. 2012:61:539–542. https://doi.org/10.1093/sysbio/sys029.

Sanderson MJ. R8s: inferring absolute rates of molecular evolution and divergence times in the absence of a molecular clock. *Bioinformatics*. 2003:19:301–302. https://doi.org/10.1093/bioinformatics/19.2.301.

Schneider H *et al.* Ferns diversified in the shadow of angiosperms. *Nature*. 2004:428:553–557. https://doi.org/10.1038/nature02361.

Schneider H *et al.* Are the genomes of royal ferns really frozen in time? Evidence for coinciding genome stability and limited evolvability in the royal ferns. *New Phytol*. 2015:207:10–13. https://doi.org/10.1111/nph.13330.

Shu J, Zhang Y, Huang T, Yan Y. The chromosome-level genome assembly of Broad-Leaf Fern (*Dipteris shenzhenensis*). *Sci Data*. 2025:12:475. https://doi.org/10.1038/s41597-025-04812-4.

Simão FA, Waterhouse RM, Ioannidis P, Kriventseva EV EMZ. BUSCO: assessing genome assembly and annotation completeness with single-copy orthologs. *Bioinformatics*. 2015:31:3210–3212. https://doi.org/10.1093/bioinformatics/btv351.

Soltis PS, Marchant DB, Van de Peer Y, Soltis DE. Polyploidy and genome evolution in plants. *Curr Opin Genet Dev*. 2015:35:119–125. https://doi.org/10.1016/j.gde.2015.11.003.

Soltis PS, Soltis DE, Savolainen V, Crane PR, Barraclough TG. Rate heterogeneity among lineages of tracheophytes: integration of molecular and fossil data and evidence for molecular living fossils. *Proc Natl Acad Sci U S A*. 2002:99:4430–4435. https://doi.org/10.1073/pnas.032087199.

Stanke M, Morgenstern B. AUGUSTUS: a web server for gene prediction in eukaryotes that allows user-defined constraints. *Nucleic Acids Res*. 2005:33:W465–W467. https://doi.org/10.1093/nar/gki458.

Sun J *et al.* OrthoVenn3: an integrated platform for exploring and visualizing orthologous data across genomes. *Nucleic Acids Res*. 2023:51:W397–W403. https://doi.org/10.1093/nar/gkad313.

Sun P *et al.* WGDI: a user-friendly toolkit for evolutionary analyses of whole-genome duplications and ancestral karyotypes. *Mol Plant*. 2022:15:1841–1851. https://doi.org/10.1016/j.molp.2022.10.018.

Szöllősi GJ, Rosikiewicz W, Boussau B, Tannier E VD. Efficient exploration of the space of reconciled gene trees. *Syst Biol*. 2013:62:901–912. https://doi.org/10.1093/sysbio/syt054.

Tang D *et al.* Genome evolution and diversity of wild and cultivated potatoes. *Nature*. 2022:606:535–541. https://doi.org/10.1038/s41586-022-04822-x.

Tang H, Bowers JE, Wang X, Ming R, Alam M AHP. Synteny and collinearity in plant genomes. *Science*. 2008:320:486–488. https://doi.org/10.1126/science.1153917.

Tarailo-Graovac M, Chen N. Using RepeatMasker to identify repetitive elements in genomic sequences. *Curr Protoc Bioinformatics*. 2009:25:4.10.11–14.10.14. https://doi.org/10.1002/0471250953.bi0410s25.

Testo W, Field A, Barrington D. Overcoming among-lineage rate heterogeneity to infer the divergence times and biogeography of the clubmoss family Lycopodiaceae. *J Biogeog*. 2018:45:1929–1941. https://doi.org/10.1111/jbi.13373.

Testo WL *et al.* Deep vicariance and frequent transoceanic dispersal shape the evolutionary history of a globally distributed fern family. *Am J Bot*. 2022:109:1579–1595. https://doi.org/10.1002/ajb2.16062.

Tong H *et al.* Fatty acyl-CoA reductase influences wax biosynthesis in the cotton mealybug, *Phenacoccus solenopsis* Tinsley. *Commun Biol*. 2022:5:1108. https://doi.org/10.1038/s42003-022-03956-y.

Van de Peer Y, Ashman TL, Soltis PS, Soltis DE. Polyploidy: an evolutionary and ecological force in stressful times. *Plant Cell*. 2021:33:11–26. https://doi.org/10.1093/plcell/koaa015.

Van Konijnenburg-Van Cittert JHA. Ecology of some late triassic to early cretaceous ferns in eurasia. *Rev Palaeobot Palynol*. 2002:119:113–124. https://doi.org/10.1016/S0034-6667(01)00132-4.

Vitte C, Panaud O. LTR retrotransposons and flowering plant genome size: emergence of the increase/decrease model. *Cytogenet Genome Res*. 2005:110:91–107. https://doi.org/10.1159/000084941.

Wang J *et al.* Allopolyploid speciation accompanied by gene flow in a tree fern. *Mol Biol Evol*. 2020:37:2487–2502. https://doi.org/10.1093/molbev/msaa097.

Wang Y *et al.* MCScanX: a toolkit for detection and evolutionary analysis of gene synteny and collinearity. *Nucleic Acids Res*. 2012:40:e49. https://doi.org/10.1093/nar/gkr1293.

Wang Y *et al.* Four near-complete genome assemblies reveal the landscape and evolution of centromeres in Salicaceae. *Genome Biol*. 2025:26:111. https://doi.org/10.1186/s13059-025-03578-7.

Weng JK, Chapple C. The origin and evolution of lignin biosynthesis. *New Phytol*. 2010:187:273–285. https://doi.org/10.1111/j.1469-8137.2010.03327.x.

Wessler SR. Transposable elements and the evolution of eukaryotic genomes. *Proc Natl Acad Sci U S A*. 2006:103:17600–17601. https://doi.org/10.1073/pnas.0607612103.

Winnepenninckx B, Backeljau T, De Wachter R. Extraction of high molecular weight DNA from molluscs. *Trends Genet*. 1993:9:407. https://doi.org/10.1016/0168-9525(93)90102-N.

Wolter KE. Lignins: occurrence, formation, structure and reactions. *For Sci*. 1973:19:160. https://doi.org/10.1093/forestscience/19.2.160.

Wu G *et al.* Shaded habitats drive higher rates of fern diversification. *J Ecol*. 2025:113:1200–1208. https://doi.org/10.1111/1365-2745.70026.

Wu T *et al.* clusterProfiler 4.0: a universal enrichment tool for interpreting omics data. *The Innovation*. 2021:2:100141. https://doi.org/10.1016/j.xinn.2021.100141.

Xiang D, Li G. Control of leaf development in the water fern *Ceratopteris richardii* by the auxin efflux transporter *CrPINMa* in the CRISPR/Cas9 analysis. *BMC Plant Biol*. 2024:24:322. https://doi.org/10.1186/s12870-024-05009-4.

Xu Z, Wang H. LTR_FINDER: an efficient tool for the prediction of full-length LTR retrotransposons. *Nucleic Acids Res*. 2007:35:W265–W268. https://doi.org/10.1093/nar/gkm286.

Yang Z. PAML 4: phylogenetic analysis by maximum likelihood. *Mol Biol Evol*. 2007:24:1586–1591. https://doi.org/10.1093/molbev/msm088.

Yi Z, Liu Y, Meert JG. A true polar wander trigger for the Great Jurassic East Asian Aridification. *Geology*. 2019:47:1112–1116. https://doi.org/10.1130/G46641.1.

Zhang Q *et al.* Blue light regulates secondary cell wall thickening via MYC2/MYC4 activation of the NST1-directed transcriptional network in *Arabidopsis*. *Plant Cell*. 2018:30:2512–2528. https://doi.org/10.1105/tpc.18.00315.

Zwaenepoel A, Van de Peer Y. Inference of ancient whole-genome duplications and the evolution of gene duplication and loss rates. *Mol Biol Evol*. 2019:36:1384–1404. https://doi.org/10.1093/molbev/msz088.